https://doi.org/10.30799/jnst.247.19050407 J. Nanosci. Tech. - Volume 5 Issue 4 (2019) 769–772

Share Your Innovations through JACS Directory

Journal of Nanoscience and Technology

Visit Journal at http://www.jacsdirectory.com/jnst

ISSN: 2455-0191

Synthesis and Characterization of Fe-TiO_2 and $NiFe_2O_4$ Nanoparticles and Its Thermal Properties

Tentu Manohra Naidu, P.V. Lakshmi Narayana*

Department of Nuclear Physics, Andhra University, Visakhapatnam – 530 003, Andhra Pradesh, India.

ARTICLEDETAILS

Article history:
Received 07 May 2019
Accepted 28 May 2019
Available online 12 June 2019

Keywords:
Fe-TiO_2 NPs
$NiFe_2O_4$ NPs
XRD

ABSTRACT

In the present research work metal-doped metal oxide nanoparticles like iron doped nanoparticles (Fe-TiO_2 NPs) and a nickel ferrite nanoparticle ($NiFe_2O_4$ NPs) were synthesized using precipitation method. The NPs were characterized by X-ray powder diffraction (XRD), Fourier-transform infrared spectroscopy (FTIR), field emission scanning electron microscopy (FESEM), and high-resolution transmission electron microscopy (HRTEM). The aim of this study is to investigate the nanoparticle thermal properties on the thermal gravimetric analysis and Cone-calorimetric analysis. The TGA results of NPs could enhance the thermal stability of the composite at 1200 °C by forming high residual char. The cone calorimeter data clearly showed that good results of heat Release rate (PHRR) and total heat Release (THR) values. The all of the obtained results conclude that metal doped metal oxide NPs were good thermal resistance inorganic fillers.

1. Introduction

Nowadays Nanotechnology is very impartment subject of research involving physics, chemistry and biotechnology. Nanoparticles were playing a key role in developing new pharmaceutical drugs and their smart delivery in selected tissue and organism [1, 2]. The widespread use of nanoparticles raised the eyebrows of the many scientists to utilize their versatile applications within the fields of aeronautics, agriculture and health sciences [3]. The advantage of nanoparticles over different material is their measurement and higher availability of surface area and lighter in weight. Engineered nanoparticles are widely used in many fields due to their widespread applications and are expected to be released in the environment [4, 5].

Nanoparticles these days have been used to prepare the nanocomposites for the improvement in fire retardant properties. The major concern of these substances is dispersion. The surface modification is essential for nanoparticles to achieve better compatible and homogeneous dispersion [6]. Dynamic mechanical thermal analysis (DMTA) was frequently used in nanocomposites characterization since it allows the measurement of stiffness and energy losses as a function of temperature [7-9]. DMTA data are strongly affected by the degree and the scale of dispersion of nanofillers. Thermal mechanical analysis (TMA) was mainly used to measure the coefficient of thermal expansion (CTE) of nanocomposite materials in comparison with those of the matrix [10]. Thermogravimetric analysis (TGA) has been used to analyze the effect of the introduction of nanofillers into a polymer matrix on the thermal stability of the polymer [11, 12].

2. Experimental Methods

2.1 Chemicals and Reagents

Titanium tetrachloride and Iron nitrate were obtained from Sigma Aldrich. Ferric chloride, nickel chloride AR Grade, sodium hydroxide AR grade, and hydrochloric acid AR grade were obtained from the Merck India limited. Distilled water was purified by using the Milli-Q Plus apparatus (Millipore, Bedford, MA, USA).

2.2 Preparation of Fe-TiO_2 Nanoparticles

The TiO_2 nanoparticles were prepared by the dropwise addition of 5 mL of $TiCl_4$ (Sigma Aldrich) in 100 mL distilled water containing 0.2 M HCl (AR Grade Purity- 36.6) at 5±0.5 °C and ultrasonicated for 1 hour at 82 °C and kept for 18 hours at 82 °C in a thermostat controlled oven ($TiCl_4 + 2H_2O \rightarrow TiO_2 + 4HCl$). The obtained white precipitate was washed with distilled water ten times by using a refrigerated centrifuge and finally washed with methanol. The methanol was then decanted and the precipitate (TiO_2 nanoparticles) was dried at 120 °C for 4 hours [12]. A 100 mL boiling solution of Iron nitrate (Sigma Aldrich) was added dropwise to the boiling distilled water containing 2 g of TiO_2 nanoparticles. The solution was sonicated at 100 °C about 30 min, according to the following chemical equation,

$$TiO_2\,(aqua) + Fe(NO_3)_3.9H_2O(aqua) \rightarrow Fe\text{–}TiO_2$$

The obtained brown color Fe-TiO_2 nanoparticles were washed with distilled water six times by using a refrigerated centrifuge and finally washed with methanol. The Fe-TiO_2 nanoparticles dried at 120 °C for 4 hours after decanted the methanol.

2.3 Preparation of Nickel Ferrite ($NiFe_2O_4$) Nanoparticles

$NiFe_2O_4$ nanoparticles were prepared by co-precipitation method. 50 mL of 0.2 M ferric chloride solution was taken into 250 mL glass beaker, and then 0.1 M nickel chloride solution was added into the same beaker. This mixture was stirred at room temperature for 2 hours to form a homogeneous solution. The pH of the solution was constantly observed as the 3 M sodium hydroxide solution was added dropwise. The reactants were consistently stirred using a magnetic stirrer until a pH level of >12.5 was achieved. A specified amount of oleic acid was added to the solution as the surfactant. The liquid precipitate was then brought to a reaction temperature of 80 °C and stirred for 1 hour. The product was cooled to room temperature and then washed twice with deionized water and ethanol to eliminate unwanted impurities and the residual surfactant from the prepared sample. Finally, the sample was centrifuged and then dried at 80 °C. The acquired substance was then ground into a fine powder.

2.4 Characterization of Fe-TiO_2 Nanoparticles

The room temperature XRD profile of the synthesized Fe-TiO_2 nanoparticles was obtained to the crystal structure and phase purity of the sample the crystallite size was calculated from the XRD spectrum using "Debye Scherrer" equation. The transform infrared (FT-IR) spectrum is

*Corresponding Author:pvl.nuclearphysics@gmail.com(P.V. Lakshmi Narayana)

https://doi.org/10.30799/jnst.247.19050407

recorded on JASCO, FT/IR-6300 FT-IR spectrometer in KBr pellets. The characterization of Fe-TiO_2 nanoparticles by FESEM (TESCAN, CZ/MIRA I LMH) showed the development of iron on the titanium matrix. The size of the particle was observed to be 10-15 nm by HRTEM (FEI, TECNAI G2 TF20-ST).

2.5 Characterization of $NiFe_2O_4$ Nanoparticles

The room temperature XRD profile of the synthesized $NiFe_2O_4$ nanoparticles was obtained to the crystal structure and phase purity of the sample the crystallite size was calculated from the XRD spectrum using "Debye Scherrer" equation. The transform infrared (FT-IR) spectrum is recorded on JASCO, FT/IR-6300 FT-IR spectrometer in KBr pellets. The characterization of $NiFe_2O_4$ nanoparticles by FESEM (TESCAN, CZ/MIRA I LMH) showed the development of Nickel on the iron matrix. The size of the particle was observed to be 6-7 nm by HRTEM (FEI, TECNAI G2 TF20-ST).

2.6 Thermal Gravimetric Analysis Test

Thermal stability of all coating formulations was performed using SDT Q600 V20.9 Build-20 instrument with 30 °C/min of the heating rate at a temperature range of 30-1200 °C under nitrogen atmosphere at the flow rate of 20 mL/min. For this analysis purpose, each sample weight was taken about 10 mg.

2.7 Combustion Test

The combustion parameters of all samples were performed on cone calorimeter in accordance with ISO 5660-2002 standard method by exposing 50 kW/m^{-2} of external heat flux. For this analysis purpose, each sample weight was taken about 5 mg.

3. Results and Discussion

3.1 Description of Fe-TiO_2 Nanoparticles

The XRD of the Fe-TiO_2 was investigating its crystalline phase by scanning from 3° to 50°. Fig. 1 indicates (peak at 27° or 31°) that it is rutile phase due to three (rutile, anatase and brookite) naturally occurring phases of titania. The calculated average crystallite size, D is 10.15 ± 0.5 nm. Using Scherer's equation. The FESEM image of Fe-TiO_2 nanoparticles presented in Fig. 2 and the average size of the particle were observed to be 40-50 nm by TEM (Fig. 3). The Fourier transform Infrared Spectroscopy was showed a broad peak can be seen at 3427 cm^{-1}, assigned to stretching vibration mode of the OH groups within the TiO_2. The stretching vibrations of the O-H groups were also observed at 1637 cm^{-1}. The peak at 2285 cm^{-1} indicated for molecular water, Ti-O-Fe stretching vibration band The bands near 498cm^{-1} was assigned to bending vibration of Ti–O bond. The FTIR spectra presented in Fig. 4.

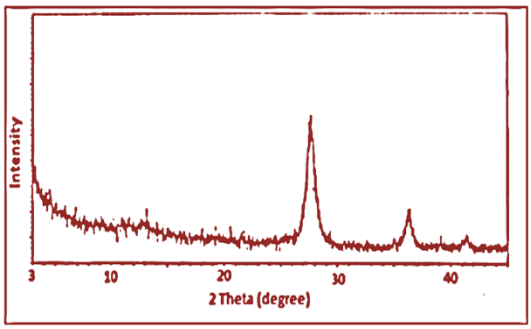

Fig. 1 XRD pattern of Fe-TiO_2 nanoparticles

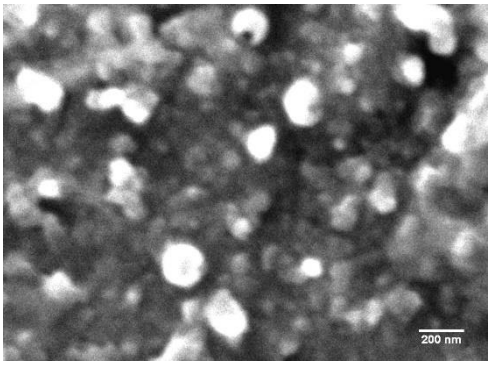

Fig. 2 FESEM Image of Fe-TiO_2 nanoparticles

https://doi.org/10.30799/jnst.247.19050407

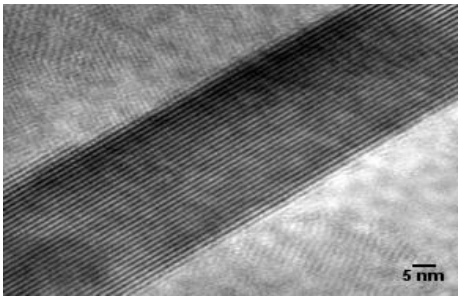

Fig. 3 The HRTEM image of Fe-TiO_2 nanoparticles

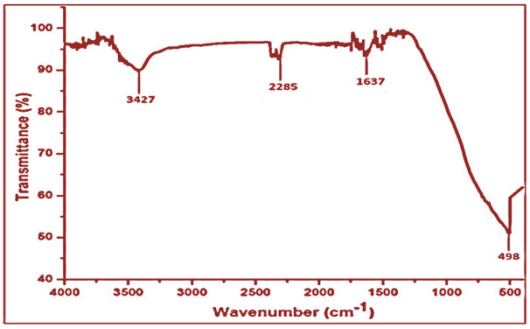

Fig. 4 FT-IR Spectra of Fe-TiO_2 nanoparticles

3.2 XRD Study for $NiFe_2O_4$ Nanoparticles

The powder X-ray pattern recorded for the sample of $NiFe_2O_4$ is shown in Fig. 5. It is consistent with the standard pattern cubic spinel structure of bulk $NiFe_2O_4$ JCPDS (Card No. 10-0325). The lattice parameter of $NiFe_2O_4$ is a = 8.339 Å, which is close to the one reported in the previous literature [29]. Extra reflections are not detected in the X-ray diffraction pattern. The calculated average crystallite size, D is 7.3 ± 1.2 nm using Scherer's equation.

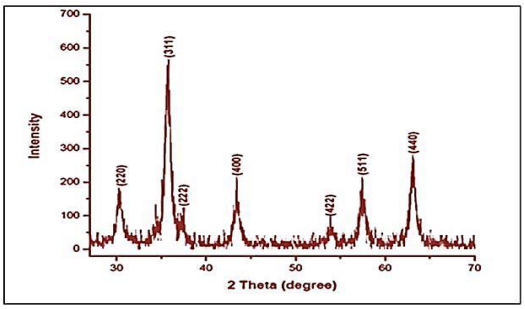

Fig. 5 XRD pattern of $NiFe_2O_4$ nanoparticles

3.3 FT-IR Study for $NiFe_2O_4$ Nanoparticles

The FTIR spectrum was observed the frequency range of 4000-500 cm-1 as shown in Fig. 6. The band located at 3403 cm^{-1} could is attributed to the symmetric vibration of –OH groups. The two main metal–oxygen bands at 673 cm^{-1} and 554 cm^{-1} are observed in the FT-IR spectrum of the synthesized $NiFe_2O_4$ samples. These two bands are usually assigned to vibration of ions in the crystal lattices. At 1362 cm^{-1} there is a significant change in the irrelevant peak of – CH bending band. The 1317 cm^{-1} peak is attributed to the characteristic $–CH_3$ bending.

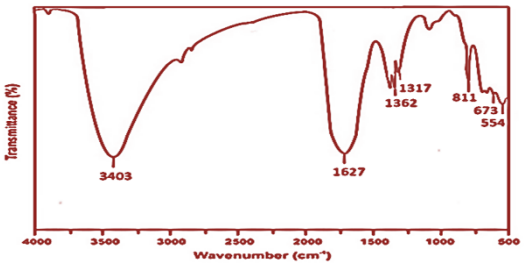

Fig. 6 FTIR spectra of $NiFe_2O_4$ NPs

3.4 FESEM Analysis of $NiFe_2O_4$ Nanoparticles

FESEM of $NiFe_2O_4$composite is shown in Fig. 7. These results show the development of Ni on iron oxide matrix. SEM micrograph depicts that the

samples contain a micrometrical aggregation of tiny particles. The existence of high dense agglomeration indicates that pore-free crystallites are present on the surface. The FESEM images show the agglomerated form of $NiFe_2O_4$ nanoparticles. As the nanoparticles possess high surface energies, they tend to agglomerate and grow into larger assemblies.

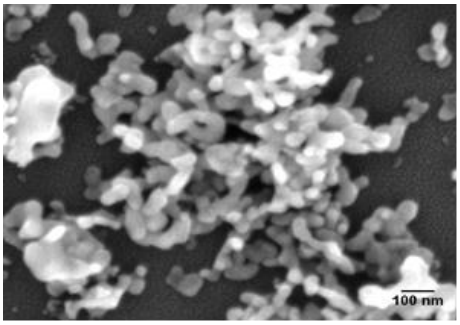

Fig. 7 FESEM image of $NiFe_2O_4$ NPs

3.5 HRTEM Analysis of $NiFe_2O_4$ Nanocomposite

The average size of the particle was observed to be 10 ± 0.5 nm as calculated from (TEM). The HRTEM micrograph (Fig. 8).

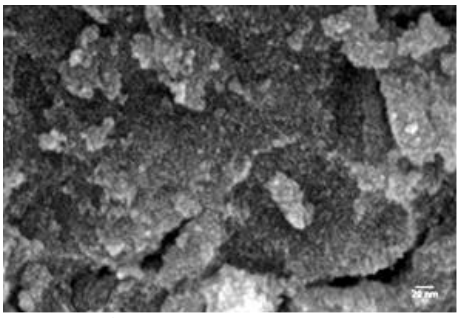

Fig. 8 The HRTEM image of $NiFe_2O_4$ NPs

Table 1 Thermal stability results of the NPs

NPs	Temp. (5% onset)	Decomposition Temp. (max)	Char residue (%) at 1200 °C
Fe-TiO2	151.45	505	57.54
$NiFe_2O_4$	149.23	501	50.02

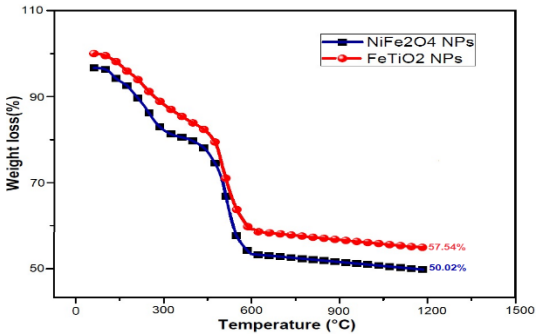

Fig. 9 TGA curve of NPs

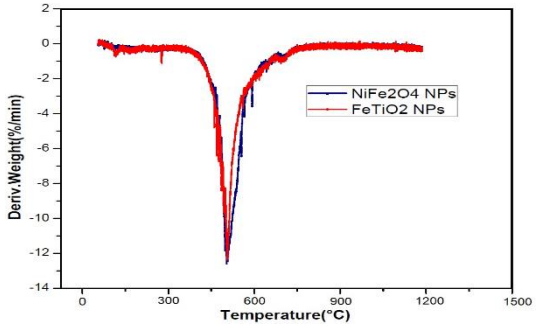

Fig. 10 DTG curve of NPs

3.6 Thermo-Gravimetric Analysis of NPs

The mass loss of a sample with respect to increasing in temperature can be evaluated by thermo-gravimetric analysis and it gives the information regarding the char formation, degradation behavior and thermal stability of the sample. The TGA and DTG curves of the NPs are represented in Table 1 and Figs. 9 and 10. The Fe-TiO_2 NPs and $NiFe_2O_4$ NPs were showed a great amount of char at 1200 °C is 57.54% and 50.02% respectively. This result indicates that the synthesized NPs were thermally more stable. From the DTG curve, decomposition occurs at 489 to 510 °C temperature range. At this step, the weight loss has occurred due to the thermal decomposition macromolecular backbone structure.

3.7 Cone-Calorimetric Analysis

The combustion study of a sample can be performed by cone calorimeter based on oxygen consumption principle. Cone calorimetric analysis provides the information for Peak heat release rate (PHRR) and total heat release (THR). The PHRR, THR values are regarded as an important indicator to characterize the flammability of material in a fire situation. The PHRR, THR curves of NPs are shown in Figs. 11 and 12 and Table 2.

Table 2 Cone calorimeter results of the NPs

NPs	PHRR (kW m^{-2})	THR (MJ m^{-2} kg^{-1})
Fe-TiO2	208.15	112
$NiFe_2O_4$	260.23	56

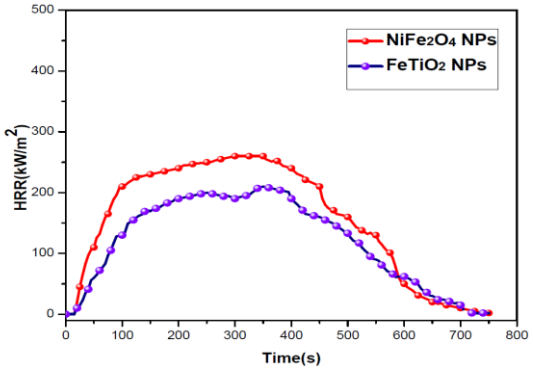

Fig. 11 PHRR curves of NPs

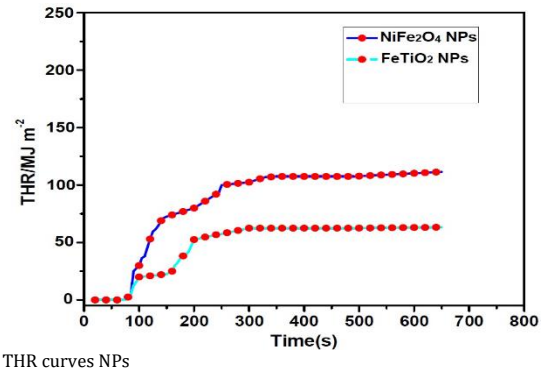

Fig. 12 THR curves NPs

4. Conclusion

TGA was established here as a viable measurement tool for nanoparticle analysis with repeatability on the order of typical TGA experiments, similar results to conventional TGA in terms of oxidation temperature and residual mass measurements in nanoparticles. The PHRR peak of the functionalized $NiFe_2O_4$ NPs was more than Fe-TiO_2 NPs due to the melting point of TiO_2 higher than Ni.

References

[1] Gerko Oskam, Metal oxide nanoparticles synthesis, characterization and application, J. Sol-Gel Sci. Tech. 37 (2006) 161-164.

[2] Siti Hajar Othman, Suraya Abdu Rashid, Tinia Idaty Mohd Ghazi, Norhafizah Abdullah, Fe-doped TiO_2 nanoparticles produced via MOCVD synthesis, characterization, and photocatalytic activity, J. Nanomater. 2011 (2011) 1-8.

[3] I. Ganesh, P. Kumar, K. Gupta, S.C. Sekhar, K. Radha, et al., Preparation and characterization of Fe-doped TiO_2 powders for solar light response and photocatalytic applications, Proces. Appl. Ceram. 6 (2012) 21-36.

[4] H. Sun, Y. Bai, Y, Cheng, W. Jin, N. Xu, Preparation and characterization of visible- light- driven carbon-sulfur codoped TiO_2 photocatalysts, Ind. Eng. Chem. Res. 45 (2006) 4971-4976.

https://doi.org/10.30799/jnst.247.19050407

[5] Marta Lezner, Ewelina Grabowska, Adriana Zaleska, Preparation and photocatalytic activity of iron-modified titanium dioxide photocatalyst, Physicochem. Probl. Miner. Proces. 48 (2012) 193-200.
[6] F. Bauera, H.J. Glasela, E. Hartmanna, H. Langgutha, R. Hinterwaldner, Functionalized inorganic/organic nanocomposites as new basic raw materials for adhesives and sealants, Int. J. Adhes. Adhes. 24 (2004) 519-522.
[7] S. Sagadevan, Investigation of the preparation and characterization of Fe-doped TiO_2 nanoparticles, J. Material. Sci. Eng. 4 (2015) 1-4.
[8] A. Leszczynska, K. Pielichowski, Application of thermal analysis methods for characterization of polymer/montmorillonite nanocomposites, J. Therm. Anal. Calorim. 93 (2008) 677–687.
[9] C. Esposito Corcione, A. Cavallo, E. Pesce, A. Greco, A. Maffezzoli, Evaluation of the degree of dispersion of nanofillers by mechanical, rheological and permeability analysis, Polym. Eng. Sci. 51 (2011) 1280-1285.
[10] E. Verdonck, K. Schaap, L.C. Thomas, A discussion of the principles and applications of modulated temperature DSC, Int. J. Pharm. 192 (1999) 3-25.
[11] L. Priya, J.P. Jog, Polyvinylidene fluoride/clay nanocomposites prepared by melt intercalation: Crystallization and dynamic mechanical behavior studies, Polym. Phys. 40 (2002) 1682-1689.
[12] W.B. Xu, H.B. Zhai, H.Y. Guo, Z.F. Zhou, N. Whitely, W.P. Pan, Application of thermal analysis methods for characterization of polymer/montmorillonite nanocomposites, J. Therm. Anal. Calorim. 78 (2004) 101-107.

https://doi.org/10.30799/jnst.247.19050407

Cite this Article as: Tentu Manohra Naidu, P.V. Lakshmi Narayana, Synthesis and characterization of Fe-TiO_2 and $NiFe_2O_4$ nanoparticles and its thermal properties, J. Nanosci. Tech. 5(4) (2019) 769–772.